PAPER *Special Issue on Concurrent Systems and Hybrid Systems*

Modeling and Simulation of Fission Yeast Cell Cycle on Hybrid Functional Petri Net

Sachie FUJITA[†], **Mika MATSUI**[†], **Hiroshi MATSUNO**[††], ***and*** **Satoru MIYANO**[†††], ***Members***

SUMMARY Through many researches on modeling and analyzing biological pathways, Petri net has recognized as a promising method for representing biological pathways. Recently, Matsuno *et. al.* (2003) introduced hybrid functional Petri net (HFPN) for giving more intuitive and natural biological pathway modeling method than existing Petri nets. They also developed Genomic Object Net (GON) which employs the HFPN as a basic architecture. Many kinds of biological pathways have been modeled with the HFPN and simulated by the GON. This paper gives a new HFPN model of "cell cycle of fission yeast" with giving six basic HFPN components of typical biological reactions, and demonstrating the method how biological pathways can be modeled with these HFPN components. Simulation results by GON suggest a new hypothesis which will help biologist for performing further experiments.

key words: *hybrid functional Petri net, Genomic Object Net, biological pathways, cell cycle, simulation*

1. Introduction

Petri net [30] is a description method for modeling concurrent systems mainly used so far to model artificial systems such as manufacturing systems [28] and communication protocols [35]. The first attempt to use Petri net for modeling biological pathways was made by Reddy *et al.* [29] which gave a method of representation of metabolic pathways. Hofestädt expanded this method to model metabolic networks [12]. After their works, several enhanced Petri nets have been used for modeling the behaviors of biological phenomena. Genrich *et al.* [7] modeled metabolic pathways with the colored Petri net with assigning enzymatic reaction speeds to the transitions, and simulated a chain of these reactions quantitatively. Voss *et al.* used the colored Petri net in different way, accomplishing a qualitative analysis of steady state in metabolic pathways [34]. The stochastic Petri net has been applied to model a variety of biological pathways; the ColE1 plasmid replication [9], the response of σ_{32} transcription factor to a heat shock [31], and the interaction kinetics of a viral invasion [32]. On the other hand, we have shown that the gene regulatory network of λ phage can be more naturally modeled as a hybrid system of "discrete" and "continuous" dynamics [15] by employing hybrid Petri net (HPN) architecture [2], [5]. It is also observed [8] that biological pathways can be handled as hybrid systems, e.g. protein concentration dynamics behaves continuously being coupled with discrete switches; protein production is switched on or off depending on the expression of other genes, i.e. presence or absence of other proteins in sufficient concentration.

Recently, by extending the notion of HPN, Matsuno *et al.* [16] introduced hybrid functional Petri net (HFPN) in order to give more intuitive and natural modeling method for biological pathways than these existing Petri nets. Furthermore, we have been developing a software "Genomic Object Net" for modeling and simulating biological pathways based on the notion of the HFPN. GON equips the GUI specially designed for biological pathway modeling.

With GON, we have modeled and simulated many biological pathways, including the gene switch mechanisms of λ phage [15], the gene regulation for circadian rhythm in *Drosophila* [16], the signal transduction pathway for apoptosis induced by the protein Fas [16], the glycolytic pathway in *E.coli* with the *lac* operon gene regulatory mechanism [17], and Notch-Delta signaling mechanism of *Drosophila* [18].

From the nature of Petri net in visualization based description method, Petri net is acceptable modeling method of biological pathways even for researchers in biology who are not familiar with mathematical descriptions and programming. On the other hand, a biological pathway consists of a variety of biological reactions. Although our previous papers above gave a number of HFPN models of biological pathways, correspondence between biological reactions and HFPN components were not described explicitly. This paper presents "HFPN component based modeling method", which will help these researchers to construct their intended biological pathways more easily. Moreover, since, with this method, researchers in biology and researchers in system engineering can share their knowledge, it is expected that this method promotes collaboration between these researchers in different fields in discovering new biological hypothesis which can not be produced without a help of computer simulation.

As an example for demonstrating the HFPN com-

Manuscript received January 1, 2000.
Manuscript revised January 1, 2000.
Final manuscript received January 1, 2000.

[†]The author is with Graduate School of Science and Engineering, Yamaguchi University
[††]The author is with Faculty of Science, Yamaguchi University
[†††]The author is with Human Genome Center, Institute of Medical Science, University of Tokyo

ponent based modeling method, this papar uses a biological mechanisms "cell cycle of fission yeast [1]." Tyson's group has constructed several ordinary differential equation models of fission yeast cell cycle [4], [24], [25], in which at most twenty proteins participate. Although they carried out numerical simulations and analyzed the properties of the cell cycle system, around 10 known proteins were left behind in their models and simulations. In contrast, we have constructed the fission yeast cell cycle model so that it contains all proteins so far examined biologically. Since fission yeast is the most examined living organism on cell cycle mechanisms, it can be said that the HFPN model of this paper is the largest cell cycle model among the existing cell cycle models.

2. Modeling Biological Pathway with Hybrid Functional Petri Net

2.1 Hybrid functional Petri net: extension of hybrid Petri net for modeling biological reactions

Petri net is a network consisting of *place*, *transition*, *arc*, and *token*. A place can hold tokens as its content. A transition has arcs coming from places and arcs going out from the transition to some places. A transition with these arcs defines a firing rule in terms of the contents of the places where the arcs are attached.

Hybrid Petri net (HPN) [2] has two kinds of places discrete place and continuous place and two kinds of transitions, discrete transition and continuous transition. A discrete place and a discrete transition are the same notions as used in the traditional discrete Petri net [30]. A continuous place can hold a nonnegative real number as its content. A continuous transition fires continuously at the speed of a parameter assigned at the continuous transition. The graphical notations of a discrete transition, a discrete place, a continuous transition, and a continuous place are shown in Fig. 1, together with three types of arcs. A specific value is assigned to each arc as a weight. When a normal arc is attached to a discrete/continuous transition, w tokens are transferred through the normal arc, in either of normal arcs coming from places or going out to places. Note that, by assigning different weights to these incoming and outgoing arcs, different amounts can be flowed in these two arcs. An inhibitory arc with weight w enables the transition to fire only if the content of the place at the source of the arc is less than or equal to w. For example, an inhibitory arc can be used to represent repressive activity in gene regulation. A test arc does not consume any content of the place at the source of the arc by firing. For example, a test arc can be used to represent enzyme activity, since the enzyme itself is not consumed.

Hybrid dynamic net (HDN) [5] has a similar structure to the HPN, using the same kinds of places and transitions as the HPN. The main difference between HPN and HDN is the firing of continuous transition. As described above, for a continuous transition of HPN, the different amounts of tokens can be flowed through the two types of arcs, coming from/going out the continuous transition. In contrast, the definition of HDN does not allow to transfer different amount through these two types of arcs. However, HDN has the following firing feature of continuous transition which HPN does not have; "the speed of continuous transition of HDN can be given as a function of values in the places".

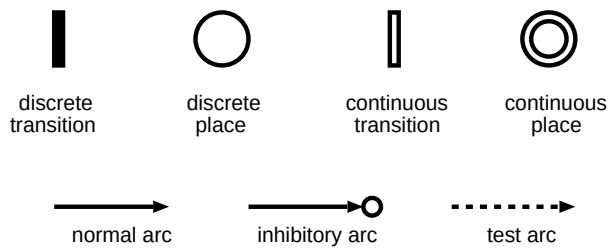

Fig. 1 Basic elements of HPN, HDN, and HFPN

From the above discussion, it can be said that each of HPN and HDN has its own feature for the firing mechanism of continuous transition. As a matter of fact, both of these features of HPN and HDN are essentially required for modeling common biological reactions. This motivated us to propose hybrid functional Petri net (HFPN) [16] which includes both of these features of HPN and HDN. Moreover, HFPN has the third feature for arcs, that is, a function of values of the places can be assigned to any arc. This feature was originated from the idea in the paper [13] which was introduced in order to realize the calculation of dynamic biological catalytic process on Petri net based biological pathway modeling.

In fact, for any continuous transition in the biological pathway model of fission yeast described in Section 3, same amount of tokens flow in the incoming and outgoing arcs to/from the transition. This means that this fission yeast model uses only feature of HDN. However, in the following, we will use the notation HFPN in order to keep consistency with the biological pathway models so far constructed [15]–[17].

2.2 HFPN components for basic biological reactions

Many biological pathways can be constructed by mainly using the following six basic reactions: (1) protein composition and decomposition, (2) enzymic reaction, (3) protein disintegration, (4) state switching, (5) state changing, and (6) substance migration. HFPN components of these reactions are listed in Fig. 2, and reaction speeds of these reactions are summarized in Table 3.1. The variables a, b, $c1$, $c2$, d, e, and f are constants. Depending on the speed of biological reactions to be modeled, the appropriate integer in the

range of 5 to 20 is assigned to each of six variables. The variables V_{max}, K_m, and K_i are the maximum speeds, a Michaelis constant, and a blocking constant of a Michaelis-Menten equation [1], respectively. In our model, we let $V_{max} = 2$ and $K_m = 1$, and use a real number in the range of 0.4 to 0.5 for the K_i.

In addition, a continuous transition with only one output arc to a continuous place (e.g., the continuous transitions Ts attached to the continuous places Cig1, Cig2, Rum1, Cdc18, and SCF_Pop1/Pop2 in Fig. 7) is used to model constant protein production.

3. Modeling Cell Cycle of Fission Yeast with the HFPN

Fig. 3 shows a whole HFPN model of the cell cycle regulation pathway of fission yeast. All initial values of places and firing speeds of continuous transitions and delay times of discrete transitions are tuned manually with repeating simulations until concentration behaviors of proteins correspond to the biological facts. Note that it is hard to decide optimal values of these parameters, since data from biological experiments are very insufficient to determine them.

Four blocks of the figure correspond to Fig. 4, Fig. 5, Fig. 6, and Fig. 7. Small part at the central-right side of this figure, which is not involved in any of these four blocks, represents the phases of cell cycle. That is, when the place G1 has token(s), the cell cycle is in G1 phase. The places S, G1, and G2 have similar meaning to the place G1. If the places off_M and off_S have token(s), the cell cycle is not in the phases M and S, respectively. When the place DNA_replication (DNA_replication_end) gets token(s), DNA replication begins (ends).

For expressing the reaction that the protein Cig1 is produced only in the G1/S phase, the test arc is used from the place G1 to the transition representing the production of the protein Cig1 (refer to Fig. 7). It is known that the S phase does not begin unless the protein Cdc18 is broken down [22], [23]. The test arc from the place representing the breakdown of Cdc18 to the transition DT_{15} is used to express this. Firing the transition DT_{15} means that the cell cycle changes from the G1 phase to the S phase.

3.1 MPF regulation

Fig. 4 shows the HFPN model of MPF regulation mechanism of budding yeast. A biological picture describing this MPF regulation is found in the URL [36].

Protein complex formation (Fig. 2 (a))

It is known that the proteins Cdc2 and Cdc13 form a complex [26]. Complex formations can be modeled by constructing an HFPN model described in Fig. 2 (a). Based on this, the complex formation is constructed with the places Cdc2, Cdc13, and Cdc2/Cdc13 at the left side in Fig. 4. The reaction speed of this complex formation is given by $\frac{[\mathsf{Cdc2}]*[\mathsf{Cdc13}]}{20}$ with referring Table 1 [†]. The transitions d_1, d_2, and d_3 are used for representing degradation of the proteins and the complex, which are attached to the places Cdc13, Cdc2, and Cdc13/Cdc2, respectively. According to Table 1, the degradation speeds are given by the formula $\frac{[\mathsf{P}]}{100}$, where [P] denotes the content of a place P at which the transition for degradation is attached. The transitions T_1 and T_3 are used for productions of the proteins Cdc13 and Cdc2, respectively. The speeds of these transitions are set to 1.

The remaining part of Fig. 4 were modeled by same manner as described above. That is, a continuous place of HFPN is placed for each substance, and places are connected by transitions and arcs whose parameters (weights of arcs and speeds of transitions) are determined based on the corresponding biological reactions. At transitions labeled with the symbol T in Fig. 4, production rates of the corresponding proteins are assigned. In the following, transitions labeled with the symbols T or d have the same meaning as above. The transitions v_1, v_{17}, v_{18}, and v_{19} of Fig. 4 are used for complex formations as shown in Fig. 2 (a).

Enzymic Reactions (Fig. 2 (b))

Transitions v_2, v_3, v_5, v_7, v_8, v_9, v_{10}, v_{11}, v_{20}, v_{21}, v_{22}, v_{23}, v_{24}, and v_{60} are classified into the following three categories according to the enzymic reaction types as shown in Table 1.

(Non-constant concentration) Although proteins MPF, CAK, and Cdc25 works as enzyme, activation level of these proteins are not always constant. Based on this fact, the formulas for non-constant concentration in Table 1 are used for the transitions v_8, v_9, v_{10}, and v_{60}.

(Constant concentration) The formula for constant concentration in Table 1 was used for the transitions v_2, v_3, v_5, v_7, v_{11}, v_{20}, v_{22}, and v_{23}, since concentrations of kinases corresponding to these transitions keeps almost constant level. The place Pyp3 represents the protein Pyp3 which back up the protein Cdc25 [21].

(Competitive inhibition) For the transitions v_{21} and v_{24}, the formulas for competitive inhibition in Table 1 were used from the following reasons. The transition v_{21} represents the reaction that inhibits the protein Cdc25 from becoming non-active by the protein PP2A which keeps almost constant concentration level throughout the cell cycle [14]. The transition v_{24} represents the reaction that convert the lamin into the lamina as the active MPF is broken down [1].

[†] [P] represents the content of a place P.

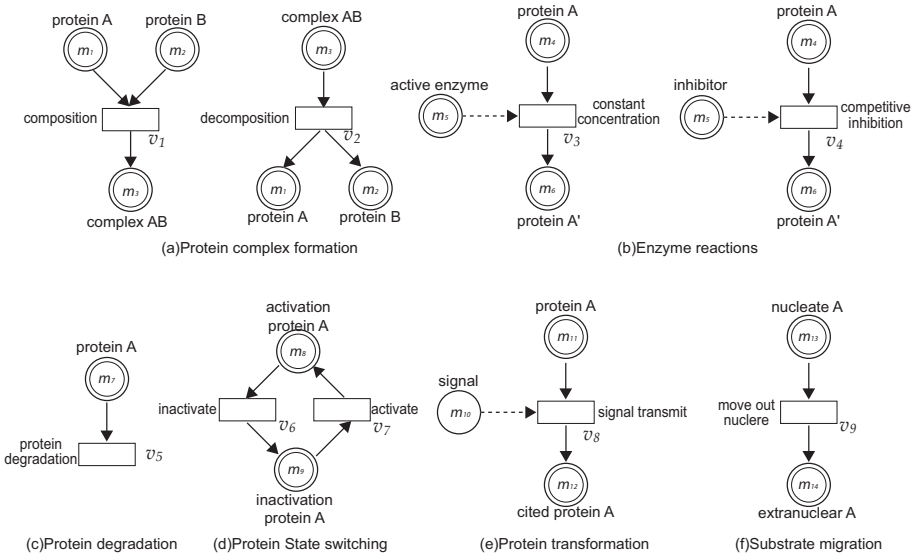

Fig. 2 HFPN components for typical biological reactions. Contents of continuous places represent concentrations of substances such as proteins. (b) Test arc is used for an enzymic reaction, since enzymes are not consumed by reactions. Two types of enzymic reactions "activating enzyme" and "blocking enzyme" are described. Furthermore, activating enzyme reactions can be classified into two patterns "constant concentration" and "variable concentration." Reaction speeds of them are given in Table 1. (e) Discrete elements can be used for state changing reactions instead of constant elements. In this case, when a place gets a number of tokens enough to fire the transition, the reaction proceeds.

Table 1 Transition speeds for HPN components of typical biological reactions in Fig. 2

Reaction		Transition speed
protein formation	composition	$v_1 = \frac{m1*m2}{a}$
	decomposition	$v_2 = \frac{m3}{a}$
enzymic reactions	non-constant concentration	$v_3 = \frac{m4*m5}{b}$
	constant concentration	$v_3 = \frac{V_{max}*m4}{K_m+m4}$
	competitive inhibition	$v_4 = \frac{V_{max}*m5}{K_m(1+\frac{m6}{K_i})+m5}$
protein degradation		$v_5 = \frac{m7}{d}$
protein state switching		$v_6 = \frac{m8}{c1}$ $v_7 = \frac{m9}{c2}$
protein transformation		$v_8 = \frac{m11}{e}$
substrate migration		$v_9 = \frac{m13}{f}$

Protein degradation (Fig. 2 (c))

At transitions labeled with the symbol d in Fig. 4, degradation rates of the corresponding proteins are assigned. For the variable d, we should choose an integer not greater than any other variables, since the speed of protein disintegration should be slower than any other reactions. Accordingly, 100 is used for the variable d in our model.

Protein state switching (Fig. 2 (d))

State of some proteins will be switched between active and non-active state depending on the concentration of other protein. Each of the following combinations of transitions (v_4, v_5), (v_{21}, v_{22}), (v_{23}, v_{24}), and (v_6, v_7, v_8) constitutes the state switching shown in Fig. 2 (d). Basically, transition speeds are assigned according to the reaction speeds given in Table 1. However, if some enzymic reaction relates to a state switching of protein, a formula for the enzymic reaction will be used. For example, for the protein Wee1, it can be considered that both activation by the MPF and non-activation by the Nim1 are enzymic reactions. Thus, formulas for enzymic reaction are used for the transitions v_7 and v_8.

Protein transformation (Fig. 2 (e))

The state of a protein will be transformed by reactions such as phosphorylation and ubiquitination [1]. For example, a part of HFPN in Fig. 4 consisting of the places Cdc13/Cdc2+2P, Cdc13/Cdc2+3P, and active_CAK and the transition v_9 represents the reaction which transforms the protein complex Cdc13/Cdc2+2P to Cdc13/Cdc2+3P by the phosphorylation with the active CAK.

Substance migration (Fig. 2 (f))

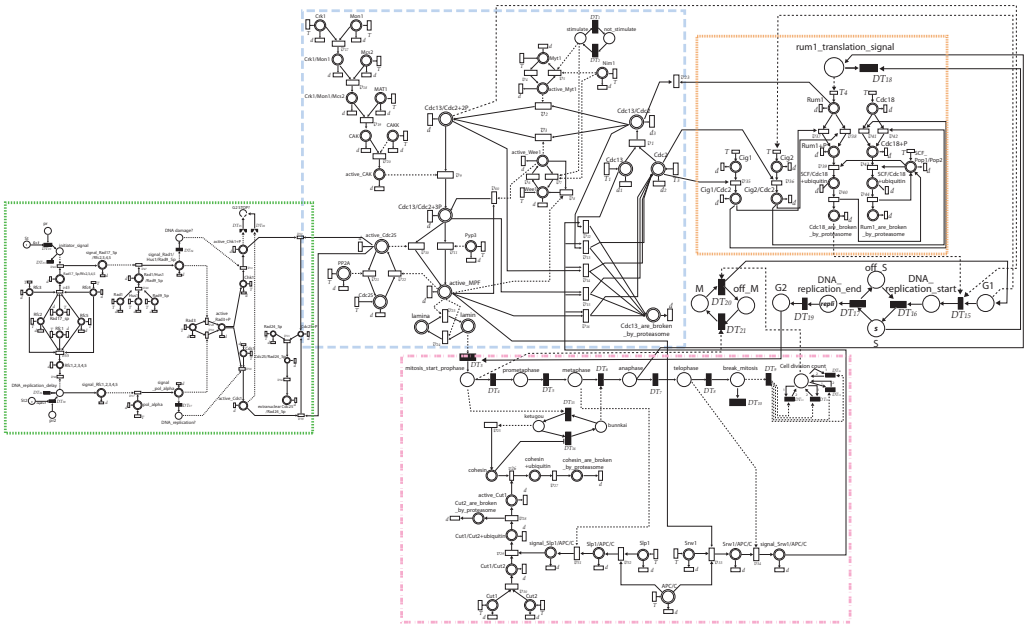

Fig. 3 A whole HFPN model of the budding yeast cell cycle regulation

This reaction is not included in Fig. 4, but used in the model of checkpoint mechanism of Fig. 5. Refer to the next subsection.

Usage of discrete elements

The transitions v_5 and v_7 are enzymic reactions with the protein Num1 and the protein complex active MPF. Although it is known that each of these reactions does not occur without a stimulation, the detail mechanism of the stimulation is still unclear. In such case, discrete elements are used. At the top-left part of Fig. 4, two discrete places and two discrete transitions constitute a part which can represents two states stimulate and not_stimulate. At each of the transitions DT_1 and DT_2, the time for state changing is assigned.

3.2 Checkpoint mechanism

The concept of checkpoint was defined by Hartwell *et al.* in 1989 [10] as follows. "*The events of the cell cycle of most organisms are ordered into dependent pathways in which the initiation of late events is dependent on the completion of early events. Control mechanisms enforcing dependency in the cell cycle are here called checkpoints.*"

Several checkpoint systems are known to work in the cell cycle. Among them, we will focus on the system of "S/M checkpoint" which coordinates the DNA synthesis and the beginning of chromosome separation. The steps of S/M checkpoint system are the following;

1. the checkpoint mechanism is started by an *initiator signal* such as ultraviolet rays radiation,
2. the *sensor* senses an abnormal status in a cell triggered by the initiator signal, and

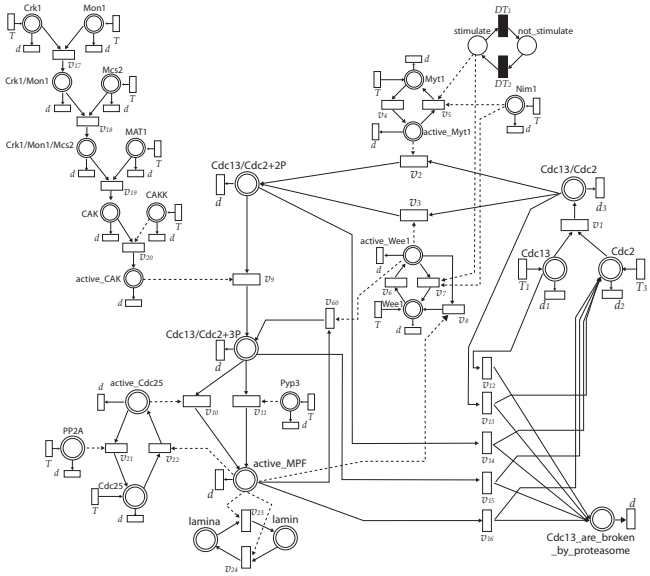

Fig. 4 HFPN model for MPF regulation

3. the *transducer* mediates the abnormal status to the *effector* or the *target*.

In Fig. 5, two checkpoint mechanisms of fission yeast "DNA damaging checkpoint" and "DNA replication checkpoint" are described together with the part of MPF activation mechanism of Fig. 4. In the following, only the mechanism for the DNA damaging checkpoint is explained, since these two mechanisms have similar structures.

The initiator signal is generated at the beginning of S-phase only when the DNA is damaged. This logic of initiator signal is realized with discrete elements at

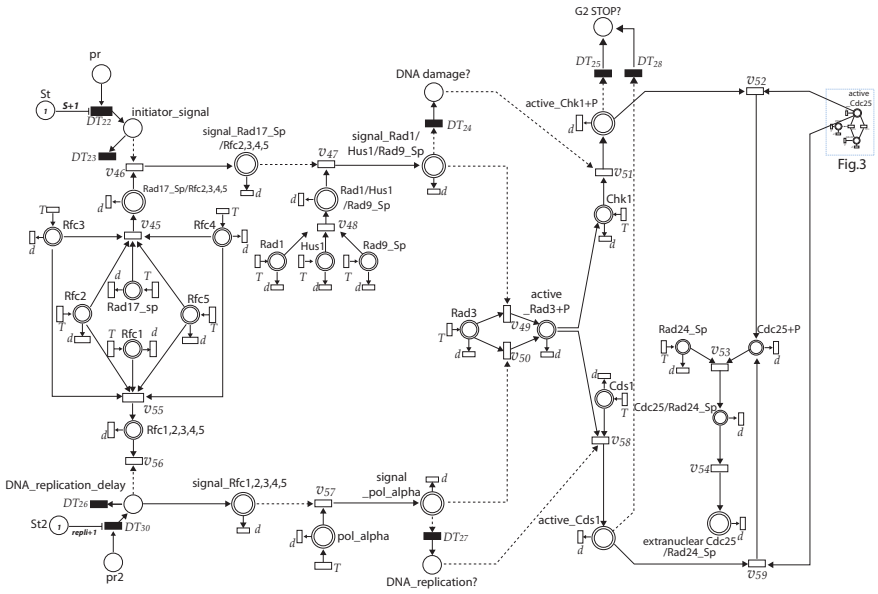

Fig. 5 HFPN model of checkpoint mechanism

the top-left corner of Fig. 5. The content of the discrete place pr represents the DNA damaging status (1:damaged, 0:not damaged). Note that the formula $S+1$ is assigned at the inhibitory arc attached to the place pr. Since the content of the discrete place is always set at 1, the place initiator_signal can get token only when the discrete place S in Fig. 3 has at least one token, where the place S indicates whether the cell cycle is in S-phase ([S]=1) or not ([S]=0).

When the concentration of the protein complex Rad17^{Sp}, Rfc2, -3, -4, -5 (place Rad17_Sp/Rfc2,3,4,5) exceeds some fixed level after detecting the initiator signal (transition v_{46} and the place signal_Rad17_Sp/Rfc2,3,4,5), the signal of DNA damaging is passed to the protein complex Rad1/Hus1/Rad9^{Sp} (the places Rad1/Hus1/Rad9_Sp and signal_Rad1/Hus1/Rad9_Sp, and the transition v_{47}). By transmitting this signal to the protein kinase Rad3 (the place Rad3), this kinase is activated through the phosphorylation (the place active_Rad3+P). The activated Rad3 phosphorylates the protein Chk1 (the place Chk1), activating this protein (the place active_Chk1+P). Note that the protein complex Rad1/Hus1/Rad9^{Sp} and the proteins Rad3 and Chk1 are *transducers*.

The *effector* in this pathway is the protein Cdc25, which is inactivated by the activated Chk1 (the place active_Chk1+P) through the phosphorylation (the transition v_{52}). The inactivated Cdc25 (the place Cdc25+P) is captured by the mobilizing factor Rad24^{Sp} (the place Rad24_Sp. Since the captured Cdc25 (the place Cdc25/Rad24_Sp) is transported to the outside of nucleus, separating from the MPF[†], it lose the ability to dephosphorize the Tyr15 site. Eventually, the cell cycle is stopped at G2-phase. By watching the discrete place DNA_damage? (G2_STOP?), we can know the status of the signal propagation of DNA damaging (the status of cell cycle termination at G2-phase).

3.3 HFPN models for the M-phase progress and the CKI effect on MPF

Chromosome segregation and cell division occur in M-phase in the order of dramatic events, prometaphase, metaphase, and anaphase. On the other hand, CDK Inhibitor (CKI) is a protein which works as a brake for the MPF, preventing the MPF being out of control from the cell cycle regulation. Rum1 is one of CKIs in yeast cell cycle, which is started to produce at the anaphase of cell cycle, being completely degraded in the S-phase. That is, accumulation of the Rum1 suppresses the MPF activation during the G1-phase.

Although both are the important processes in the cell cycle, we only present the HFPN models as shown in Fig. 6 and Fig. 7 due to the limitation of the space for this paper. Refer to the webpage [36] for the details of them.

4. Simulations by Genomic Object Net

After describing an HFPN of the biological pathway to be modeled, parameters of transition speed/delay and initial values of places have to be determined based on the biological knowledge and/or the facts described in biological literature. In general, many trial and error processes are required until appropriate parameters for simulation are determined. Since GON provides the GUI specially designed for biological pathway model-

[†]This transportation corresponds to the reaction of "substance migration" of Fig. 2 (f)

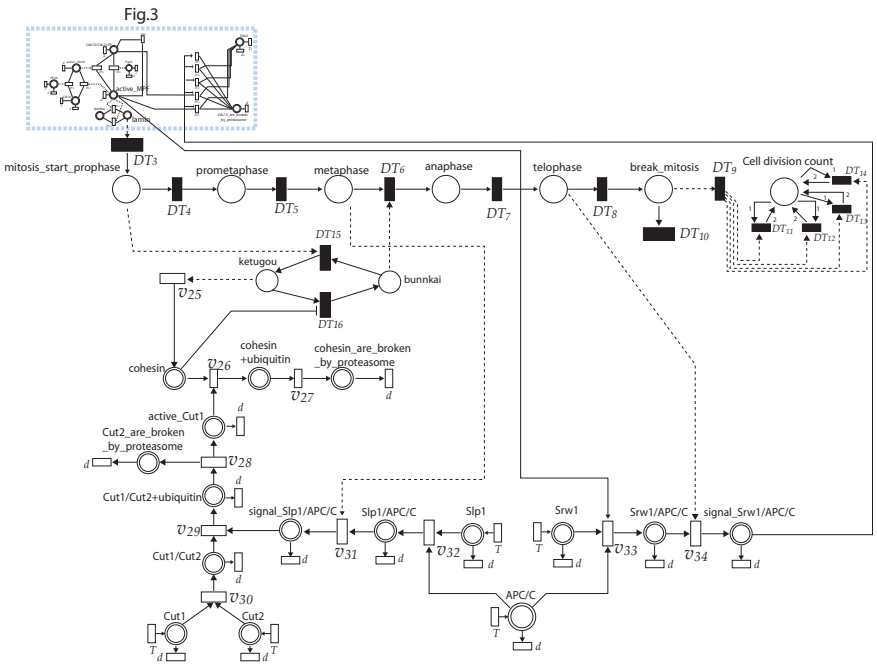

Fig. 6 HFPN model for M-phase progress

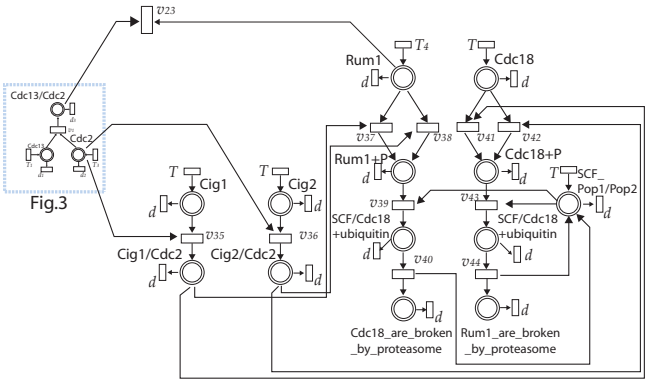

Fig. 7 HFPN model for MPF activating process and CKI effect

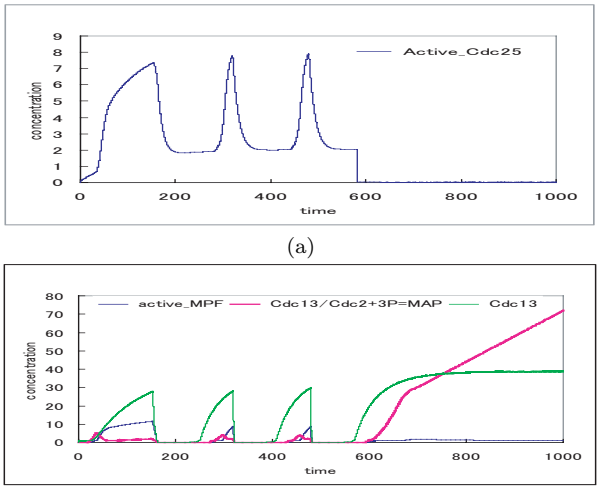

(a)

(b)

Fig. 8 Abnormal behaviors of DNA-damaged fission yeast

ing, we can perform these processes very easily and smoothly.

The constructed HFPN model of fission yeast cell cycle was simulated by using GON. With showing the simulation result of a known behavior of DNA-damaged fission yeast, the appropriateness of the constructed HFPN model is verified. In addition, we will present a new biological hypothesis obtained from the simulation with changing expression level of the protein Rum1.

4.1 Verification of the constructed model: observing behaviors of DNA-damaged fission yeast

Fig. 8 shows concentration behaviors of the proteins and protein complexes related to MPF activation, where DNA-damage occurs during a cell cycle. †

That is, as observed in Fig. 8 (a), the amount of active_Cdc25 is reduced rapidly due to the DNA-damage which was realized by putting a token in the place pr in Fig. 5 at the time around 550. The signal triggered by this action propagates to the transition v_{52} which reduces the amount of the place active_Cdc25. The mechanism of this signal propagation was explained in the

†For each of Fig. 8 (a) and (b), the first waveform has a different shape compared to the succeeding waveforms. During the period of the first waveform, values in the places converge to the values with which the succeeding waveforms repeat periodically. That is, the first waveform has to be neglected. The same situation occurs in Fig. 9 (a), (b), and (c).

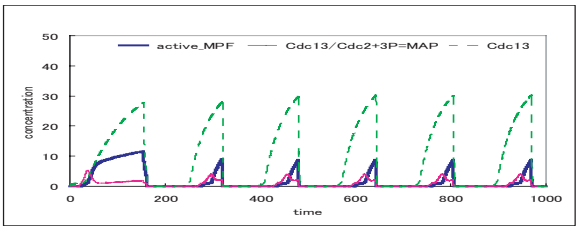

(a) wild type

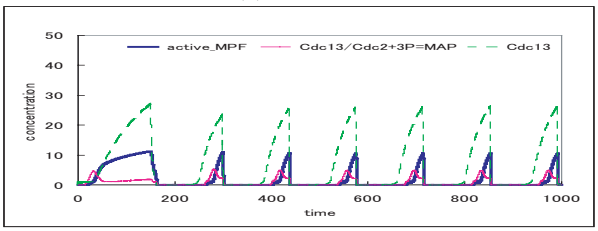

(b) deactivated

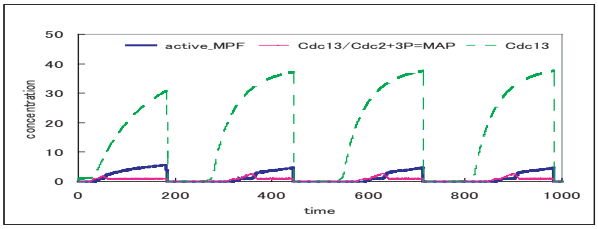

(c) over expressed weakly

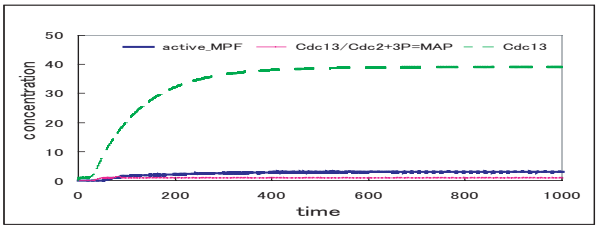

(d) over expressed strongly

Fig. 9 Simulation results of Rum1 mutants

subsection 3.2 with Fig. 5.

Fig. 8 (b) shows the behaviors of the places Cdc13, active_MPF and Cdc13/Cdc2+3P in Fig. 4. With comparing Fig. 8 (a), we can observe that both the protein Cdc13 and the MPF stop oscillating at the time of the DNA-damage. This observation reflects the biological fact that activation of the protein complex Cdc13/Cdc2 is controlled by the Cdc25 activation [1]. This simulation result supports the appropriateness of the constructed HFPN model.

4.2 Simulations of mutants: producing hypotheses for further biological experiments

Fig. 9 shows the simulation results of Rum1 mutants. The simulation result of (b) is obtained by removing the arc from the transition T_4 to the place Rum1 in Fig. 7. Furthermore, by adding the transition with the arc going into the place Rum1, the simulation results of (c) and (d) are obtained. The values 2.0 and 1.0 are assigned to the transition for the case of weak over expression (c) and strong over expression (d), respectively. Behaviors of the protein Rum1 for the figures (a)-(d) are presented in the website [36].

It is known from the biological experiments that cell cycle does not stop even when the gene *rum*1 is deactivated [3]. The simulation result of (b) supports this fact. In addition, it can be observed that the period of cell cycle of (b) is shorter than that of (a) of wild type. This observation supports the fact that the protein Rum1 controls the period of cell cycle by breaking down the complex Cdc2/Cdc13 [19].

Biological experiments in [11] elucidate the phenomenon that over-expressing of the protein Rum1 causes the arrest of the MPF activation. The simulation result of (d) supports this biological phenomenon. On the other had, the period of simulation result of (c) is longer than that of (d), suggesting that the period of cell cycle becomes longer if the over-expressing rate is decreased to some level. Note that this suggestion has not been confirmed by any biological experiment yet.

The above argument highlights that, with the help of computer simulations, biologists can effectively produce hypotheses which will guide them in performing the further biological experiments.

5. Conclusions

Researches on Petri net has a long history of nearly 40 years from the paper by Dr. Petri [27] and it is mathematically well-founded and practically well-established. Based on the researches on Petri nets, many tools have been developed by researchers in concurrent technology [37].

GON is a biosimulation tool developed with inheriting the tradition of the researches on Petri nets. These Petri net tools so far developed generally have user-friendly GUIs which allows us to describe complex concurrent systems very easily and smoothly. GON inherits this feature of Petri net, enabling to describe and manipulate biological pathway naturally even for biologists who are not familiar with mathematical description and programming language. In contrast, E-Cell [33] and Gepasi [20], which are well-known biosimulation systems, employ ordinary differential equations as description method for biological pathways. In addition, each of these systems does not equip the visual editor as GON to describe biological pathways.

In this paper, we explained how biological pathways can be described by HFPN with the example of the cell cycle of fission yeast. The constructed cell cycle pathway model was simulated by GON. The simulation results suggest that GON has very high potential to accelerate efficiencies of biological experiments drastically.

Acknowledgments

The authors would like to thank Dr. Masao Na-

gasaki and Mr. Atsushi Doi who gave us very useful and suggestive comments for simulations. This work is partially supported by the Grand-in-Aid for Scientific Research on Priority Areas "Genome Information Science" from the Ministry of Education, Culture, Sports, Science and Technology in Japan.

References

[1] B. Alberts, A. Johnson, J. Lewis, M. Raff, K. Roberts, and P. Walter, "*Molecular Biology of the Cell, Fourth Edition,*" Garland Science, 2002.

[2] H. Alla and R. David, R., "Continuous and hybrid petri nets," *Journal of Circuits, Systems, and Computers* vol.8, no.1, pp.159–188, 1998.

[3] J. Benito, C. Martin-Castellanos, and S. Moreno, "Regulation of the G_1 phase of the cell cycle by periodic stabilization and degradation of the $p25^{rum1}$ CDK inhibitor," *EMBO J.*, vol.17, no.2, pp.482–497, 1998.

[4] A. Ciliberto, B. Novak, and J.J. Tyson, "Mathematical model of the morphogenesis checkpoint in budding yeast," *Journal of Cell Biology*, Vol.163, No.6, pp.1243–1254, 2003.

[5] R. Drath, "Hybrid object nets: an object oriented concept for modeling complex hybrid systems," *Proc. Hybrid Dynamical Systems, 3rd International Conference on Automation of Mixed Processes, ADPM'98,* pp.437–442, 1998.

[6] D.L. Fisher and P. Nurse, "A single fission yeast mitotic cyclin B p34cdc2 kinase promotes both S- phase and mitosis in the absence of G1 cyclins," *EMBO J.*, vol.15, no.4, pp.850–860, 1996.

[7] H. Genrich, R. Küffner, and L. Voss, K, "Executable Petri net models for the analysis of metabolic pathways," *International Journal on Software Tools for Technology Transfer,* vol.3, no.4, pp.394–404, 2001.

[8] R. Ghosh and C. Tomlin, "Lateral inhibition through delta-notch signaling: A piecewise affine hybrid model," *Proc. 4th International Workshop on Hybrid Systems:Computation and Control, Lecture Notes in Computer Science 2034*, pp.232–246, 2001.

[9] P.J.E., Goss and J. Peccoud, "Quantitative modeling of stochastic systems in molecular biology by using Stochastic Petri nets," *Proc. Natl. Acad. Sci. USA 95,* pp.6750–6755, 1998.

[10] L.H. Hartwell, T.A. Weinert, "Checkpoints: controls that ensure the order of cell cycle events," *Science,* vol.246, pp.629–634, 1989.

[11] P.V. Jallepalli and T.J.Kelly, "Rum1 and Cdc18 link inhibition of cyclin-dependent kinase to the initiation of DNA replication in Schizosaccharomyces pombe," *Genes Dev.*, vol.10, no.5, pp.541–552, 1996.

[12] R. Hofestädt, "A Petri net application to model metabolic processes," *J. System Analysis, Modeling Simulation,* vol.16, pp.113–122, 1994.

[13] R. Hofestädt and S. Thelen, "Quantitative modeling of biochemical networks," *In Silico Biology,* vol.1, 0006, http://www.bioinfo.de/isb/1998/01/0006/, 1998.

[14] N. Kinoshita, H. Ohkura, M. Yanagida, "Distinct essential roles of type1 and 2A protein phosphatases in the control of the fission yeast cell division cycle," *Cell*, vol.63, no.2, pp.405–415, 1990.

[15] H. Matsuno, A. Doi, M. Nagasaki, and S. Miyano, "Hybrid Petri net representation of gene regulatory network," *Proc. Pacific Symp. on Biocomputing 2000*, pp.338–349, 2000.

[16] H. Matsuno, Y. Tanaka, H. Aoshima, A. Doi, M. Matsui, and S. Miyano, "Biopathway representation and simulation on hybrid functional Petri net," *In Silico Biology* , vol.3, no.3, pp.389–404, 2003.

[17] H. Matsuno, S. Fujita, A. Doi, M. Nagasaki, and S. Miyano, "Towards biopathway modeling and simulation," *Proc. ICATPN 2003 (LNCS 2679)*, pp. 3–22, 2003.

[18] H. Matsuno, R. Murakami, R. Yamane, N. Yamasaki, S. Fujita, H. Yoshimori, and S. Miyano, "Boundary formation by Notch signaling in Drosophila multicellular systems: Experimental observations and a gene network modeling by Genomic Object Net," *Proc. Pacific. Symp. on Biocomputing 2003*, pp.152–163, 2003.

[19] K. Matsuoka, N. Kiyokawa, T. Taguchi, J. Matsui, T. Suzuki, K. Mimori, H. Nakajima, H. Takenouchi, T. Weiran, Y.U. Katagiri, J. Fujimoto, "Rum1, an inhibitor of cyclin-dependent kinase in fission yeast, is negatively regulated by mitogen-activated protein kinase-mediated phosphorylation at Ser and Thr residues," *Eur. J. Biochem,*, vol.269, pp.3511–3521, 2002.

[20] P. Mendes, "GEPASI: a software for modeling the dynamics, steady states and control of biochemical and other systems," *Comput. Appl. Biosci.,* Vol.9, No.5, pp.563–571, 1993.

[21] J.B. Millar, G. Lenaers, and P. Russell, "Pyp3 PTPase acts as a mitotic inducer in fission yeast," *EMBO J.*, vol.11, no.13, pp.4933–4941, 1992.

[22] M. Muzi-Falconi, G.W. Brown, and T.J. Kelly, "cdc18+ regulates initiation of DNA replication in *Schizosaccharomyces pombe*," *Proc. Natl. Acad. Sci. U S.A.*, vol.93, issue.4, pp.1566–1570, 1996.

[23] H. Nishitani and P. Nurse, "p65cdc18 plays a major role controlling the initiation of DNA replication in fission yeast," *Cell*, vol.83, no.3, pp.397–405, 1995.

[24] B. Novak, A. Csikasz-Nagy, B. Gyorffy, K. Chen, J.J. Tyson, "Mathematical model of fission yeast cell cycle with checkpoint controls at G1/S, G2/M and metaphase/anaphase transitions," *Biophysical Chemistry*, Vol.72, pp.185–200, 1998.

[25] B. Novak, Z. Pataki, A. Ciliberto, and J.J. Tyson, "Mathematical model of the cell division cycle of fission yeast," *Chaos,* Vol.11, No.1, pp.277–286, 2001.

[26] P. Nurse, "Ordering S phase and M phase in the cell cycle," *Cell*, vol.79, no.4, pp.547–550, 1994.

[27] C.A. Petri, "Kommunikation mit Automaten," *Bonn: Institut für Instrumentelle Mathematik, Schriften des IIM Nr.3,* 1962, also, English translation, "Communication with Automata" New York : Griffiss Air Force Base, Tech. Rep. RADC-TR-65-377, vol.1, Suppl. 1, 1966.

[28] J.-M. Proth, J.-M., "Petri nets for modelling and evaluating deterministic and stochastic manufacturing systems," *Proc. 6th International Workshop on Petri Nets and Performance Models (PNPM'97)*, pp.2–15, 1997.

[29] V.N. Reddy, M.L. Mavrovouniotis, and M.N. Liebman, "Petri net representations in metabolic pathways," *Proc. The 1st International Conference on Intelligent Systems for Molecular Biology,* pp.328–336, 1993.

[30] W. Reisig, "*Petri Nets,*" Springer-Verlag, 1985.

[31] R. Srivastava, M.S. Peterson, and W.E. Bentley, "Stochastic kinetic analysis of the *Escherichia coli* stress circuit using σ_{32}-targeted antisense," *Biotechnol. Bioeng.*, vol.75, no.1, pp.120–129, 2001.

[32] R. Srivastava, L. You, J. Summers, and J. Yin, "Stochastic versus deterministic modeling of intracellular viral kinetics," *J. Theor. Biol.*, vol.218, pp.309–321, 2002.

[33] M. Tomita, K. Hashimoto, K. Takahashi, T. Shimizu, Y. Matsuzaki, F. Miyoshi, K. Saito, S. Tanida, K. Yugi, J.C. Venter, and C. Hutchison, "E-CELL:Software environment for whole cell simulation," *Bioinformatics*, Vol.15, pp.72–84, 1999.

[34] K. Voss, M. Heiner, and I. Koch, "Steady state analysis of metabolic pathways using Petri nets," *In Silico Biology,* vol.3, no.3, pp.367–387, 2003.
[35] G. Wheeler, "The modelling and analysis of IEEE802.6's configuration," *Application of Petri Nets to Communication Networks (Lecture Notes in Computer Science 1605, Billington, J., Diaz, M., and Rozenberg, G. (ed.))*, pp.69–92, 1999.
[36] *http* : *//genome.ib.sci.yamaguchi-u.ac.jp/˜gon/yeast/*
[37] *http* : *//www.daimi.au.dk/PetriNets/*